Journal of Alloys and Compounds 504 (2010) 177–180

Contents lists available at ScienceDirect

Journal of Alloys and Compounds

journal homepage: www.elsevier.com/locate/jallcom

Long lasting phosphorescence in oxygen-deficient zinc–boron-germanosilicate glass–ceramics

Geng Lin[a,b], Guoping Dong[d], Dezhi Tan[c], Xiaofeng Liu[a,b], Qiang Zhang[a,b], Danping Chen[a], Jianrong Qiu[d,*], Quanzhong Zhao[a,*], Zhizhan Xu[a,*]

[a] State Key Laboratory of High Field Laser Physics, Shanghai Institute of Optics and Fine Mechanics, Chinese Academy of Sciences, Shanghai 201800, China
[b] Graduate School of the Chinese Academy of Sciences, Beijing 100039, China
[c] State Key Laboratory of Silicon Materials, Zhejiang University, Hangzhou 310027, China
[d] Key Lab of Specially Functional Materials of Ministry of Education, and Institute of Optical Communication Materials, South China University of Technology, Guangzhou 510641, China

ARTICLE INFO

Article history:
Received 17 February 2010
Received in revised form 13 May 2010
Accepted 21 May 2010
Available online 1 June 2010

Keywords:
Long lasting phosphorescence
Glass–ceramic
Ge-related oxygen-deficient centers

ABSTRACT

Long lasting phosphorescence has been observed in oxygen-deficient zinc–boron-germanosilicate glass–ceramics after 254 nm ultraviolet lights irradiation at room temperature. Electron spin resonance (ESR) spectrum confirms the presence of two paramagnetic centers. And the ESR signal shows a synchronized decay process with afterglow intensity after removing the excitation light, suggesting the afterglow is associated with the paramagnetic centers which are generated during the irradiation. Based on the approximate t^{-1} decay law of the phosphorescence intensity, the long lasting phosphorescence is attributed to thermal assisted tunneling recombination between pairs of distant electrons and Ge-related oxygen-deficient centers.

1. Introduction

In recent years extensive research work has been carried out for developing new long lasting phosphorescence (LLP) materials because of their wide use in emergency lighting, safety indication, road signs, and so on [1–5]. Actually, LLP is a so special phenomenon due to the thermal-stimulated recombination of holes and electrons in traps at room temperature that only suitable hosts doped with right activator could yield considerable phosphorescence. In the past decades, LLP materials with superior properties have been prepared with hosts of crystalline oxides, sulfides, oxy-sulfides, and glasses activated with rare-earth (RE) as well as transition metal (TM) ions; and their emission colors cover almost the entire visible wavelength range [1–11]. However, the above-mentioned LLP materials, like many other commercial luminescent materials, all rely on various activators or co-activators, most of which are RE ions that their storages are less. The search for a non-RE doped and green material has stimulated much effort in the development of new luminescent materials with low cost and non-toxicity [12]. In this paper, we report the observation of blue LLP on oxygen-deficient zinc–boron-germanosilicate glass–ceramics. This LLP material represents a new family of glass–ceramics that is free of RE or TM. Luminescence spectra together with ESR spectra are employed to clarify the mechanism of the LLP.

2. Experimental

Colorless and transparent glass sample with composition $60ZnO–20B_2O_3–17SiO_2–3GeO_2–4Al$ (mol%) is obtained by conventional melt-quenching technique using high-purity ZnO, H_3BO_3, SiO_2, GeO_2, Al (all of 99.9% (mol%)) as raw materials. Approximately 30 g batches are mixed and then melted in an alumina crucible with an alumina cap at 1450 °C for 1 h under the ambient atmosphere. The melt is poured onto a stainless steel plate and pressed with another stainless steel plate to obtain the transparent glass sample (ZBSG-G). The ZBSG-G sample is annealed at 700 °C for 5 h to get ZBSG-C1 and at 850 °C for 5 h to get ZBSG-C2, respectively. Both ZBSG-C1 and ZBSG-C2 are opaque glass–ceramics. X-ray diffraction (XRD) patterns of the samples are obtained by Rigaku D/MAX-2550-18KW powder diffractometer with Cu Kα-radiation. Raman spectra are measured by a Renishaw inVia spectrometer with a 488 nm Ar^+ laser excitation. The excitation, emission, and phosphorescence spectra and phosphorescence decay curves are recorded by a JASCO FP-6500 spectrofluorometer. Electron paramagnetic resonance (ESR) spectra are obtained by a Bruker A30 ESR spectrometer (300 K, 9.866 GHz, X-band). All measurements are taken at room temperature.

3. Results and discussion

Fig. 1 shows the XRD patterns of the prepared samples. The broad peaks of ZBSG-G are due to the amorphous structure of the glass phase. Whereas both ZBSG-C1 and ZBSG-C2 show sharp diffractive peaks which can be ascribed to the polycrystalline

* Corresponding authors at: State Key Laboratory of High Field Laser Physics, Shanghai Institute of Optics and Fine Mechanics, Chinese Academy of Sciences, Qinghe Load 390#, Jiading, Shanghai 201800, China.
E-mail addresses: qjr@zju.edu.cn (J. Qiu), zqz@siom.ac.cn (Q. Zhao), zzxu@mail.shcnc.ac.cn (Z. Xu).

0925-8388/$ – see front matter.
doi:10.1016/j.jallcom.2010.05.080

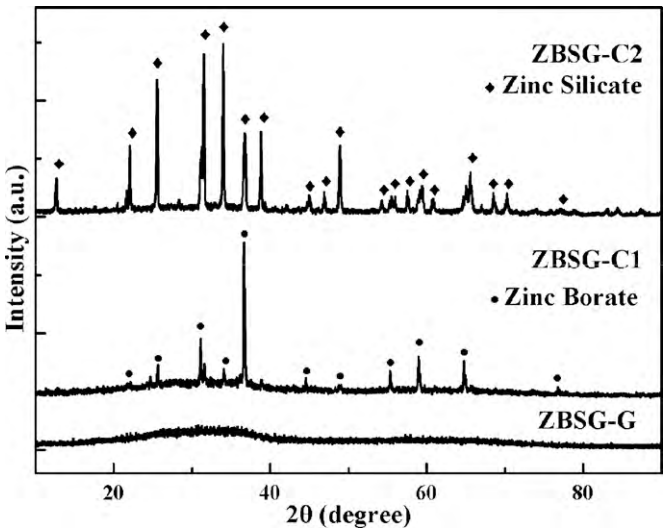

Fig. 1. XRD patterns of ZBSG samples.

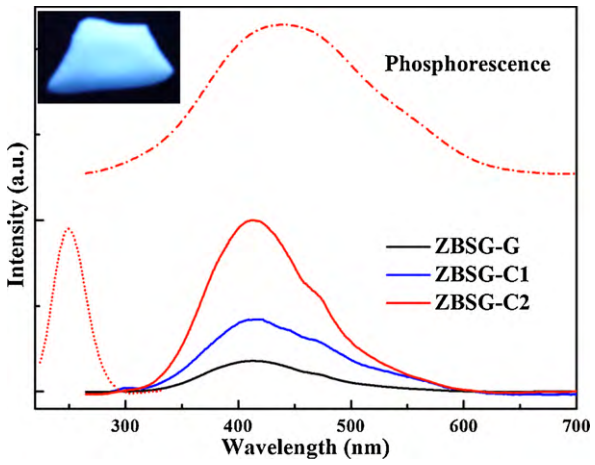

Fig. 3. Emission, excitation and phosphorescence spectra of ZBSG samples, inset shows a photo picture of the phosphorescence after an external excitation source was switched off.

phases of zinc borate and zinc silicate by comparing the XRD data of the samples with JCPDS cards. Zinc borate phase predominates in ZBSG-C1 sample, while zinc silicate predominates in ZBSG-C2 sample. This phenomenon is quite similar to that reported by Li et al. [3].

Structure of ZBSG glass and glass–ceramics are also characterized by Raman spectra, as presented in Fig. 2. In the spectrum of ZBSG-G, the bands peaking at 886, 944 and 1064 cm^{-1} are due to stretching mode of Si–O or Ge–O bands [13] and the bands peaking at 788, 1275, and 1384 cm^{-1} are due to the stretching mode of B–O band [13,14]. And in the spectra of ZBSG-C1 and C2, sharp bands with peaks at 657, 769, 790, 819, 871, 909, and 942 cm^{-1} are found. The band at 657 cm^{-1} is due to the stretching mode of Al–O in $ZnAl_2O_4$ [15], which may be ascribed to the addition of Al in the raw materials and glass melts reacted with alumina crucible during the melting process. The bands at 769, 790, 819 cm^{-1} are probably due to the stretching of ZnB_2O_4, and the bands at 871, 909, and 942 cm^{-1} are probably due to the stretching modes of Si–O in Zn_2SiO_4 [15]. This result indicates that ZnB_2O_4 phase predominates in ZBSG-C1, while Zn_2SiO_4 predominates in ZBSG-C2. This is consistent with the XRD results.

Fig. 3 shows the emission, excitation and phosphorescence spectra of the samples. As can be seen, the emission spectra have similar appearance. Only the relative intensity becomes stronger from ZBSG-G to C1 and to C2. From the XRD and Raman results we know that ZBSG-G is almost glass phase, and zinc borate polycystic phase predominates in ZBSG-C1 with a little glass phase, while zinc silicate polycystic phase predominates in ZBSG-C2. It is known that, the luminescence intensity of a luminescent center in a crystal phase is usually much stronger than that in a glass phase. Therefore, the PL intensity becomes stronger from ZBSG-G to C1 and to C2. The emission peak at 410 nm excited by 254 nm can be assigned to the triplet to singlet (T_1–S_0) transitions of the Ge-related oxygen-deficient centers (GODC) [16–18]. Furthermore, the appearance of the phosphorescence spectrum is also similar to the emission spectrum, and is confirmed to remain unchanged, while the intensity of the phosphorescence decreases with time. But we also notice that the LLP band is a little broader than PL band. This can be attributed to that longer wavelength emission which has longer lifetime, then the phosphorescence from shorter wavelength region is decayed quickly than that from longer wavelength region, which result in the LLP band broadening to longer wavelength region than PL band. However, ZBSG-G did not present LLP. And moreover, we did not observe the similar LLP phenomenon in the ZBSG glass–ceramic sample which without the GODC that produced by addition of metallic Al. Therefore, the GODC acts as luminescent center in the LLP.

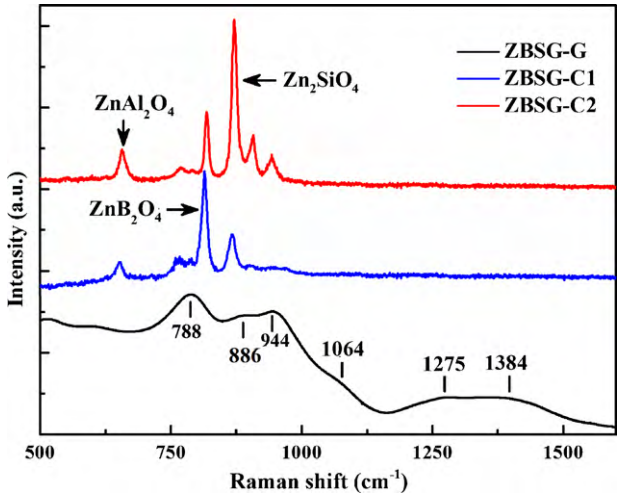

Fig. 2. Raman spectra of ZBSG samples.

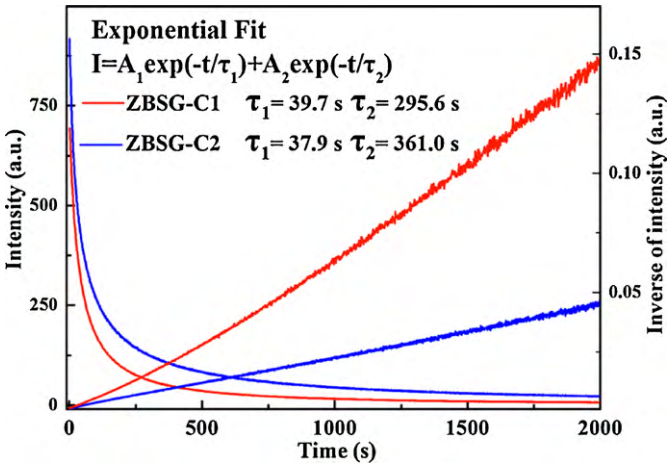

Fig. 4. Afterglow decay curves of recorded after the ZBSG glass–ceramic was irradiated with an UV lamp for 5 min.

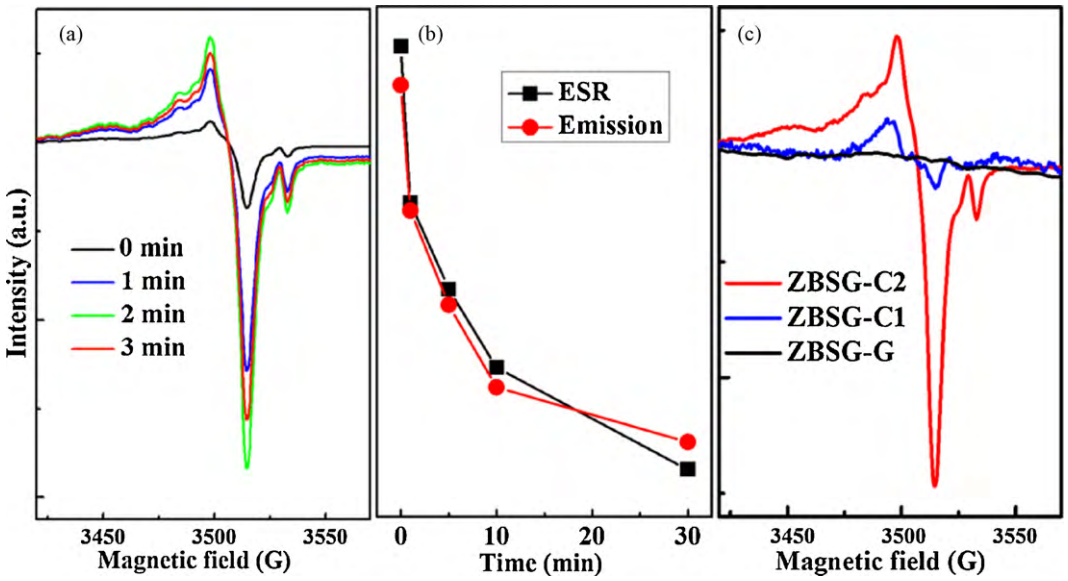

Fig. 5. (a) Time evolutions of ESR spectra of ZBSG-C2 during UV irradiation. (b) ESR and LLP intensity as a function of decay time of the ZBSG-C2 during the afterglow process. (c) ESR spectra of ZBSG samples.

Fig. 4 illustrates the decay curves of the phosphorescence monitored at 410 nm after 5 min UV light excitation at 254 nm. The intensity of the phosphorescence seems to decrease quickly at the beginning and then slowly with the passage of time. The decay curves have been analyzed by curve fitting and it is found that the curve can be fitted well by using the second-order exponential decay equation:

$$I = A_1 \exp\left(\frac{-t}{\tau_1}\right) + A_2 \exp\left(\frac{-t}{\tau_2}\right),$$

where I is the phosphorescence intensity; A_1 and A_2 are two constants; t is the time; and τ_1 and τ_2 are decay time for the exponential components. The fitting values of τ_1 and τ_2 are 39.7, 295.6 s for ZBSG-C1 and 37.9, 361.0 s for ZBSG-C2. Actually, the blue phosphorescence of ZBSG-C2 can be observed by naked eyes even 2 h after the excitation source is switched off.

Furthermore, we also found that the inverse of the phosphorescence intensities showed a nearly linear dependence on the decay time, namely, $I(t) = I_0 t^{-1}$, where I_0 is the intensity at $t = 0$. The curves of the inverse of the phosphorescence intensity versus decay time are also shown in Fig. 4. Avouris and Morgan [19] and Delbecq et al. [20] found that the phosphorescence decayed as the reciprocal of the time in KCl: AgCl (TlCl) and interpreted it as through tunneling recombination process between pairs of distant electrons and emission centers. Therefore, we suggest that the LLP of our samples are mainly due to the recombination between pairs of distant electrons and GODCs through thermally assisted tunneling.

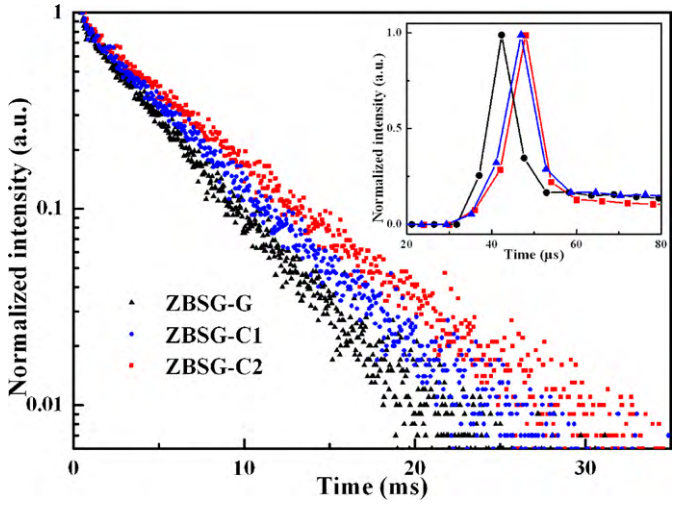

Fig. 6. Decay curves of GODC photoluminescence of ZBSG-G, C1 and C2, the inset shows the rise part of the decay curves.

For a better understanding of the mechanism for the LLP of the ZBSG glass–ceramics, ESR spectra are employed to monitor the processes of light storage during continuous excitation with an UV lamp, and light release by afterglow emission. Fig. 5a shows the time evolution of ESR spectra of ZBSG-C2 during continuous excitation with an UV lamp. The intensity of ESR grows rapidly in the initial 1 min and then tends to be saturated after only 3 min. It is clearly evident that the concentration of the paramagnetic center is increased as a result of UV irradiation, which may be caused by photon generated electrons or holes trapped at the defect centers. All the spectra have similar shape with the corresponding g values of 1.994, and 2.009. According to Ref. [21], the $g = 2.009$ is ascribed to the hole center on oxygen, and $g = 1.994$ is due to the oxygen vacancies coordinated with Zn^{2+} acts as electron trapping centers.

Likewise, the ESR spectra recorded after removal of the excitation light have similar shape and g value. Moreover, it can be observed that a rapid decrease in the intensity of the ESR occurred in the initial 3 min, and then the decay process slowed down. As shown in Fig. 5b, the ESR signal intensity as well as the emission intensity is plotted as a function of decay time. The ESR signal shows a synchronized decay process with afterglow intensity after removing the excitation light, suggesting that the afterglow is associated with the paramagnetic centers which are generated during the irradiation of ZBSG glass–ceramic with the UV lamp. The increment of the ESR intensity by photo-activation is in the sequence ZBSG-C2 > ZBSG-C1 > ZBSG-G (Fig. 5c). This can be attributed to the defects that are generated and increased during the heat treatment.

Fig. 6 shows the decay curves of the GODC photoluminescence of ZBSG-G, C1 and C2. The lifetime of ZBSG-G, C1 and C2 are 9.8, 10.6 and 12.1 ms, respectively. The lifetime of glass–ceramic sample is longer than that of glass sample. This may attribute to smaller non-radiative rate in glass–ceramic than that in glass. The inset of Fig. 6 also shows the rise part of the decay curves. The "rise time" of ZBSG-

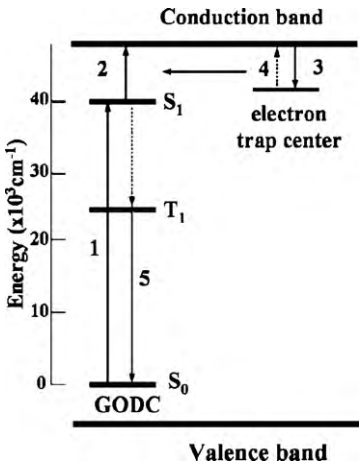

Fig. 7. Schematic energy band diagram of the ZBSG-C ceramic sample.

G, C1 and C2 are 11, 17, and 18 μs, respectively. Glass–ceramic sample has longer "rise time" than glass sample.

On the basis of the above discussion, we suggest a schematic energy band diagram (Fig. 7) for explanation. First, the transitions from the ground state of GODC (S_0) to the singlet excited state (S_1) by UV irradiation (transition 1). Then the electrons at the S_1 state could enter the conduction band easily (transition 2), making the electrons easily captured by the traps (transition 3). Then, the trapped electrons, when excited to the conduction band thermally at room temperature (transition 4), can tunnel to the nearby GODC and be captured into the excited singlet state (S_1). Finally, the characteristic luminescence occurs when this excited state decays radioactively to the ground state of GODC (transition 5).

4. Conclusions

We have observed blue long lasting phosphorescence in ZBSG glass–ceramics. The long-persistent phosphorescence is assumed to be originated from thermal assisted tunneling recombination between pairs of distant electrons and GODC, which have been confirmed by ESR, and phosphorescence decay results. The present ZBSG glass–ceramics can compete with the existing LLP materials because it is prepared by a simple procedure from cheap raw materials without use of RE ions as activators.

Acknowledgments

This work was financially supported by National Natural Science Foundation of China (Grant nos. 50672087 and 60778039), National Basic Research Program of China (2006CB806007), National High Technology Program of China (2006AA03Z304) and Changjiang Scholars and Innovative Research Team in University (IRT0651).

References

[1] M. Yamazaki, Y. Yamamoto, S. Nagahama, N. Sawanobori, M. Mizuguchi, H. Hosono, J. Non-Cryst. Solids 241 (1998) 71.
[2] Y. Lin, Z. Tang, Z. Zhang, C. Nan, Appl. Phys. Lett. 81 (2002) 996.
[3] C. Li, S. Wang, Q. Su, Mater. Res. Bull. 37 (2002) 1443.
[4] B. Liu, C. Shi, Z. Qi, Appl. Phys. Lett. 86 (2005) 191111.
[5] B. Lei, B. Li, X. Wang, W. Li, J. Lumin. 118 (2006) 173.
[6] X. Qu, L. Cao, W. Liu, G. Su, P. Wang, J. Alloys Compd. 487 (2009) 387.
[7] L. Xiao, Q. Xiao, Y. Liu, P. Ai, Y. Li, H. Wang, J. Alloys Compd. 495 (2010) 72.
[8] H. Zeng, X. Zhou, L. Zhang, X. Dong, J. Alloys Compd. 460 (2008) 704.
[9] C. Li, Q. Su, J. Alloys Compd. 408–412 (2006) 875.
[10] R. Pang, C. Li, L. Jiang, Q. Su, J. Alloys Compd. 471 (2009) 364.
[11] X. Sun, J. Zhang, X. Zhang, Y. Luo, X. Wang, J. Phys. D: Appl. Phys. 41 (2008) 195414.
[12] X. Liu, S. Ye, G. Dong, Y. Qiao, J. Ruan, Y. Zhuang, Q. Zhang, G. Lin, D. Chen, J. Qiu, J. Phys. D: Appl. Phys. 42 (2009) 215409.
[13] T. Furukawa, W.B. White, J. Mater. Sci. 16 (1981) 2689.
[14] W.L. Konijnendijk, J.M. Stevels, J. Non-Cryst. Solids 18 (1975) 307.
[15] http://rruff.info/.
[16] J. Qiu, A.L. Gaeta, K. Hirao, Chem. Phys. Lett. 333 (2001) 236.
[17] G. Lin, B. Zhu, S. Zhou, H. Yang, J. Qiu, Opt. Express 15 (2007) 16980.
[18] G. Lin, G. Dong, X. Liu, Q. Zhang, D. Chen, J. Qui, Electrochem. Solid-State Lett. 1 (2010) J1.
[19] P. Avouris, T.N. Morgan, J. Chem. Phys. 74 (1981) 4347.
[20] C.J. Delbecq, Y. Toyozawa, P.H. Yuster, Phys. Rev. B 9 (1974) 4497.
[21] H. Kawazoe, R. Suzuki, S. Inoue, M. Yamane, J. Non-Cryst. Solids 111 (1989) 16.